A CI study of the CuCO and $CuCO^+$ complexes

Manuela Merchán, Ignacio Nebot-Gil,[a] Remedios González-Luque, and Enrique Ortí
Departamento de Química Física, Facultad de Ciencias Químicas, Universitat de València, Dtor. Moliner 50, Burjassot, 46100 Valencia, Spain

(Received 6 August 1986; accepted 25 March 1987)

MO CI calculations are carried out using an optimal space of valence virtual MOs obtained by means of a projection technique, as a linear combination of the AOs which are more occupied in the molecular Fock space. Localization of the occupied MOs and nonvalence virtual MOs is also achieved. The overall procedure is proven to be quite advantageous and well suited to obtain potential energy curves which keep the same physical meaning along the range of distances studied. Using a slightly better than double-zeta quality basis set, a valence CAS-CI, and selected CI wave function by the CIPSI algorithm have revealed a possible weak van der Waals interaction for the $^2\Sigma^+$ state of CuCO, which remains when polarization functions are added to the basis set for the carbon and oxygen atoms. Even though the CuCO $^2\Pi$ and $CuCO^+$ $^1\Sigma^+$ states are energetically close, the nature of the interactions is quite different, π bonding and mainly electrostatic, respectively. The results give further support to the view of the neutral metal–CO interaction as a balance of σ repulsion and π backbonding. However, it is proposed that the driving force for the positive ion metal–CO interaction becomes essentially electrostatic.

I. INTRODUCTION

The interaction of one or more metal atoms with carbon monoxide is an area of great interest and rapid development because of its implication in many fields of current chemical research. The study of such complexes may give some insight into aspects related to homogeneous and heterogeneous catalysis, and also surface chemistry. For instance, the M/CO systems, where M represents a transition metal, are involved in important reactions such methanol,[1] methane,[2] and Fischer–Tropsch[3] sythesis. In these reactions the chemisorption of CO on several metals seems to play a fundamental role: whether the dissociation of CO is followed by hydrogenation, or hydrogenation is followed by dissociation is the key to the many mechanisms proposed.[4]

From the experimental point of view, adsorption of CO on a metal surface has been one of the more studied problems in surface chemistry. In the case of CO/Cu (100), combination of theory, employing a cluster model, with experimental data has been used to give a major understanding of the bonding of CO on a copper surface.[5]

Interaction of a copper atom with carbon monoxide presents an especially intriguing problem. Theoretical calculations[6,7,8] do not predict a bound complex for the CuCO $^2\Sigma^+$ ground state.[5] However, copper carbonyls, CuCO and $Cu(CO)_3$, have been identified by electron spin resonance spectra (ESR) generated in argon matrices as reported by Kasai and Jones.[9]

In copper monocarbonyl the semifilled copper hybrid orbital sp_σ would be pointing away from CO. Earlier, Huber *et al.*,[10] using matrix isolation infrared and UV-visible spectroscopy, obtained evidence for CuCO, $Cu(CO)_2$, $Cu(CO)_3$, and $Cu_2(CO)_6$; the CO stretching frequencies for these complexes may indicate the presence of π backdonation. Thus, the study of these carbonyls is very important, both as a potential tool for incorporation of copper into supports for catalytic purposes,[11] and especially relevant for catalytic hydrogenation of carbon monoxide to obtain methanol[1,4(c),4(i),4(j)] and of intrinsic interest by themselves for theoretical chemists.

In this paper a CI and CAS-CI study of the CuCO $^2\Sigma^+$ ground state is presented. The interaction of $Cu(^2S)$ with $CO(^1\Sigma^+)$ is expected to be weakly bound or weakly repulsive, so, special attention has been paid to build, as much as possible, size- and distance-consistent potential energy curves in order to avoid the major problems implied when working with limited CI approaches. Moreover, adequate valence virtual orbitals are used and the influence of different types of CI and basis set is analyzed. Since in both $Cu(CO)_2$ and $Cu(CO)_3$ the $Cu(^2P)$ is involved, the interaction of $Cu(^2P)$ with $CO(^1\Sigma^+)$ is also considered as preliminary to the study of $Cu_n(CO)_m$, $n = 1$, $m = 2,3$ and $n = 2$, $m = 6$. In addition, the $CuCO^+(^1\Sigma^+)$ is also studied for comparison purposes to analyze the copper–CO bond. As pointed out elsewhere,[8] the difference in stability of the neutral and ionic complexes may also be important in modelling the secondary ion mass spectra.

The paper is organized as follows. In Sec. II, we discuss the computational details of this study. We describe the basis sets used, and outline the method to obtain an adequate space of valence virtual orbitals and how the orthogonal set of occupied and virtual localized MOs has been built to perform the CI calculations. Our results for the $^2\Sigma^+$ and $^2\Pi$ states of CuCO are presented separately for each complex in Sec. III. Section IV contains the results for $CuCO^+(^1\Sigma^+)$. In Sec. V, the main variational correlation effects for these complexes are analyzed in comparison with the correspond-

[a] To whom correspondence should be addressed.

 0021-9606/87/151690-11$02.10 © 1987 American Institute of Physics

Downloaded 29 Jan 2010 to 147.156.182.23. Redistribution subject to AIP license or copyright; see http://jcp.aip.org/jcp/copyright.jsp

ing ones for isolated CO; also, the findings are related to previous work. Our conclusions are summarized in Sec. VI.

II. COMPUTATIONAL DETAILS

The SCF calculations have been carried out using the PSHONDO program,[12] a modified version of the HONDO program package[13] including the pseudopotential method of Durand and Barthelat.[14,15] Thus, the calculations have been restricted to the valence electrons of the carbon and oxygen ($2s$ and $2p$ shells), and copper ($3d$ and $4s$ shells) atoms; the helium-like and argon-like cores of carbon and oxygen, and copper, respectively, have been represented by nonempirical potential functions. Standard parameters are used for carbon and oxygen.[16] The parameters used for copper were determined by Pelissier.[17] Valence atomic basis sets of Gaussian type orbitals (GTO), optimized for the ground state of the atoms with these specific pseudopotentials, were used.[16,17] Two different types of basis sets are employed, namely, DZ and DZ + P. In the DZ basis set, the GTOs are contracted in a double-zeta form except for copper where the three s GTO are kept uncontracted in order to obtain a better description of the $4s$ orbital; the $(4s,4p/4s,4p/3s,4p,5d)$ primitive set is contracted to $(2s,2p/2s,2p/3s,2p,2d)$, where information separated by slashes belongs to the carbon, oxygen, and copper atoms, respectively. Actually, the so-called DZ basis set is slightly larger than a double-zeta basis set. The second basis set, DZ + P, introduces a set of polarization d functions in the carbon and oxygen atoms of exponents 0.7[18] and 1.25,[18] respectively, to the DZ basis.

For the complexes studied in the present work, inclusion of the correlation energy is needed since it definitively plays an important role in determining type of binding. The basis set full CI is computationally prohibitive and a partition of the correlation energy is necessary.

The full treatment of the nondynamical correlation energy,[19] i.e., correlation within the shell of valence occupied and virtual MOs, is highly desirable. An ideal way to carry out this is variationally, by the valence CASSCF procedure.[20] Unfortunately, the process can be quite expensive and the active space of MOs is frequently reduced to only a fraction of the valence part. If done in an arbitrary way, the process does not maintain all its advantages. The multiconfigurational valence complete active space (CAS) SCF procedure optimizes both the valence occupied and virtual MOs. However, the characteristics found for the occupied orbitals do in the present systems not differ significantly from the occupied MOs obtained in a monodeterminantal self-consistent-field (SCF) calculation. Thus, employing some cheaper approximate definitions of valence virtual MOs, the full valence CI can be achieved directly by a CAS-CI calculation. Then, the dynamical correlation energy can be obtained by less rigorous methods.

The problem of how to build distance-consistent potential energy curves is especially important for weakly bonded systems since the distance inconsistency of trucated CI (or of any selection) could result in an error larger than the binding energy. A practical solution proposed to this problem[21] consists in always using localized MOs, both occupied and virtual, since in that case the double excitations will always keep the same basic physical meaning, and as we show later, it becomes possible to practice distance-consistent selections.

The valence virtual MOs have been obtained through slight improvement[21] of the procedure proposed by Chambaud *et al.*,[22] consisting of the projection of the SCF atomic orbitals of the free atoms onto the virtual molecular space. The valence virtual MOs are linear combinations of the projected AOs having the largest eigenvalues coming from the diagonalization of the overlap matrix of the projected AOs, i.e., virtual MOs having essentially valence components. This procedure is very efficient and has been proven to give results almost identical to those obtained by a MCSCF calculation.[22]

The preparation for a CI calculation takes several steps. After the corresponding SCF calculation the HAOs for carbon and oxygen atoms are obtained by diagonalizing the part of the density matrix belonging to the carbon and oxygen atoms, respectively. A preliminary coefficient matrix is built by collecting the following sets of MOs: (1) First, the SCF SOMO, if any, (it is mainly the semifilled s AO of the copper atom) which was obtained by the Nesbet operator.[23] (2) The result of the projection of the HAO lone pairs onto the molecular Fock space. (3) The canonical HF occupied orbitals of the free CO projected into the molecular occupied Fock space. (4) The canonical occupied molecular orbitals of the corresponding CuCO complex are added. (5) The transformed valence virtuals MOs[22] obtained using the HAOs.[21] (6) The result of the projection of the canonical virtual molecular orbitals of the free CO into the space of canonical virtual MOs of the complex. (7) The same as (6) but with the virtual AOs of the metal. (8) In addition, the canonical virtual MOs of the complex are placed.

The set of orbitals so obtained, in this order, are orthogonalized by means of a Schmidt process. After elimination in this way of the redundant linear combinations, the result is a set of localized MOs which resemble the corresponding fragments (CO and Cu), and keep the same physical meaning, except for the orthogonalization tails, along a Cu–CO potential energy curve, with well defined MOs, lone pairs, valence, and oscillating character. The total CPU time involving in these transformations (obtaining the HAO and construction of the final matrix of molecular orbitals) is about 3% of that of an SCF calculation.

The selected CI calculations were performed with the multireferential CIPSI algorithm,[24] which proceeds by an iterative selection of the reference determinants, according to the Epstein–Nesbet definition[25] of the unperturbed Hamiltonian. The correlation energy is calculated in two parts. First, the Hamiltonian operator is built in the reference space and diagonalized, leading to the variational part of the correlation energy including the more important contributions. Secondly, all single and double excitations from the reference space are generated and their contributions to the correlation energy calculated to second order in energy using the Moller–Plesset barycentric definition[26] of the unperturbed Hamiltonian.

In this work the number of configurations (NCF) in the reference space is 30 to 74, including the effect of about

Downloaded 29 Jan 2010 to 147.156.182.23. Redistribution subject to AIP license or copyright; see http://jcp.aip.org/jcp/copyright.jsp

12×10^5–23×10^5 determinants depending on the case considered.

The optimal distances have been obtained by polynomial fitting. If it is not otherwise stated the C–O distance has been kept at the experimental value.[27]

III. RESULTS FOR THE CuCO COMPLEX

The CuCO complex in $C_{\infty v}$ symmetry implies five low-lying states correlating to the closed shell ground state of CO, $^1\Sigma^+$, and the $Cu(^2S)$, and $Cu(^2P)$ atomic states. The $^2S(3d^{10}4s^1)$ atomic configuration of copper gives a $^2\Sigma^+$ state. The $^2P(3d^{10}4p^1)$ configuration lying at 3.80 eV[27] above the ^2S generates three states, two of Π symmetry and one of Σ symmetry.

Due to the repulsion between singly ocupied 4*s* copper orbital and the highest occupied molecular orbital (HOMO) of CO, a localized lone pair on the carbon atom, the $^2\Sigma^+(4s^1)$ state of the complex is expected to give a weakly repulsive wall, as found in previous studies[6–8] or a weakly bonded van der Waals complex. This repulsion may disappear in the $^2\Pi(4p^1_{x,y})$ states[5] which may therefore induce stronger bonding. The $^2\Sigma^+(4p_z)$ state should be higher than the two last ones, due to a stronger repulsion between the $4p_z$ and the carbon lone pair, and in fact the nature of this bond should be quite similar to the $^2\Sigma^+(4s^1)$. The more interesting states are the $^2\Sigma^+(4s^1)$ and $^2\Pi(4p^1_{x,y})$ ones, dealing with a different type of interaction, weak and strong, respectively, and therefore implying different type of bonding. For that reason, in what follows, we present the results separately: Part A is concerned with the CuCO $^2\Sigma^+$ state and part B with the CuCO $^2\Pi$ state.

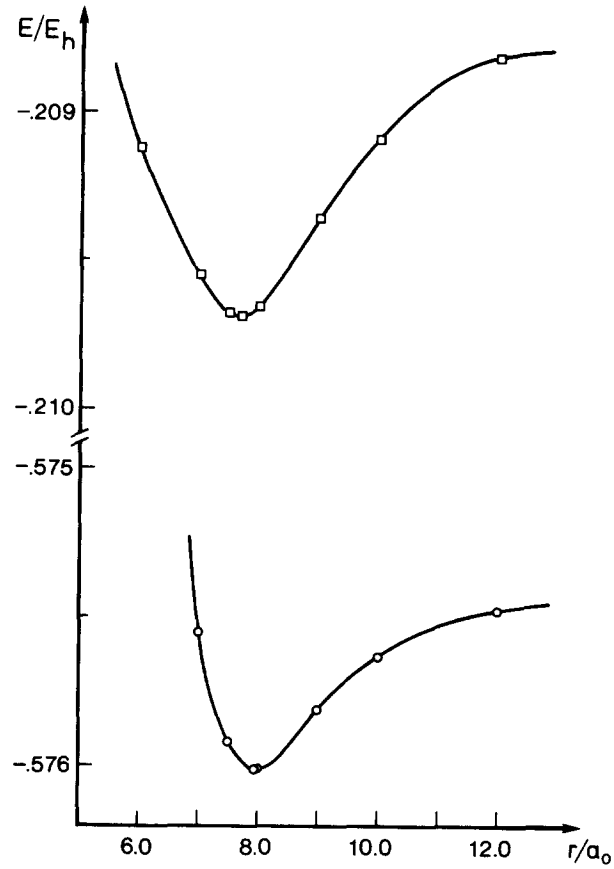

FIG. 1. Variational (upper part, □) and second-order corrected (lower part, ○) CAS–CI (NCF = 142) potential energy curves vs r(Cu–C), for the CuCO $^2\Sigma^+$ state, using the DZ basis set. The energies are relative to $-71.000\,00\,E_h$.

A. CuCO $^2\Sigma^+$ state

At a qualitative level, one notices that the canonical occupied MOs obtained from the RHF calculation of the complex, taking as trial vectors the corresponding eigenvectors of the fragments $Cu(^2S)$ and $CO(^1\Sigma^+)$, are quite unperturbed with respect to the isolated fragments. Once the localization procedure on the doubly occupied MOs has been carried out, the following MOs are clearly identified: lone pairs on the carbon and oxygen atoms, n_C and n_O; $\sigma_{C\text{-}O}$, the carbon–oxygen σ bond; four π orbitals, the two $(\pi_{C\text{-}O})$,*x*,*y* MOs and the d_{xz}, d_{yz} belonging to the copper atom; two δ MOs, $d_{x^2-y^2}$ and d_{xy} of copper. The HOMO is mainly a Cu $4s^1$ with a little participation of the copper p_z orbital: $s-\lambda p_z$, with a slight polarization away from the CO carbon lone pair. This orbital is unchanged from the Nesbet procedure,[23] since the open shell is not mixed with the doubly occupied MOs. Three valence virtuals MOs are determined: the σ^* and $\pi^*_{x,y}$ MOs of CO.

Firstly, a valence CAS-CI calculation is done within the set of bonding MOs and their antibonding counterparts, using the DZ basis set. In the present calculation seven active MOs are considered, *s* on Cu, and $\sigma,\pi,\sigma^*,\pi^*$ of CO, which make a total of 142 determinants. Two e^- of opposite spins in each π subsystem and three e^- in the active σ MOs are maintained, discarding for technical reasons the two septuple excitations. Modifying the Cu–C distance in the range from 4.0 to 12.0 a_0, a shallow potential energy curve was obtained, showing a minimum at 7.695 a_0 (see Fig. 1). When the CAS is perturbed to the second order in energy in a Rayleigh–Schrödinger Moller–Plesset perturbation expansion, the optimal Cu–C distance is displaced to a slightly longer distance 7.978 a_0, the interaction energy being less pronounced.

As Fig. 2 shows, a weakly bound minimum is also obtained using the other multireference zeroth-order wave function, which is perturbed to the same level in the CIPSI algorithm.[24] The reference space obtained at 4.0 a_0 has been used to build the potential energy curve in order to keep the same basic information at all points of the curve which can be ensured by the procedure used (see Sec. II). The optimal distances are 8.461 and 7.611 a_0, obtained by diagonalization of the Hamiltonian built on the 63 most important determinants selected iteratively, and including the second order perturbation corrections from single and double excitations of the reference space, respectively. In the latter case, there is a more pronounced depth. On the other hand, comparison of Figs. 1 and 2 put forward the efficiency of multireferential methods such as CIPSI, since a lesser number of determinants recovers, variationally, a larger part of the correlation energy.

Since we are dealing with weak intermolecular interactions, we have improved the basis set by adding polarization functions on the carbon and oxygen atoms, i.e., using the

Downloaded 29 Jan 2010 to 147.156.182.23. Redistribution subject to AIP license or copyright; see http://jcp.aip.org/jcp/copyright.jsp

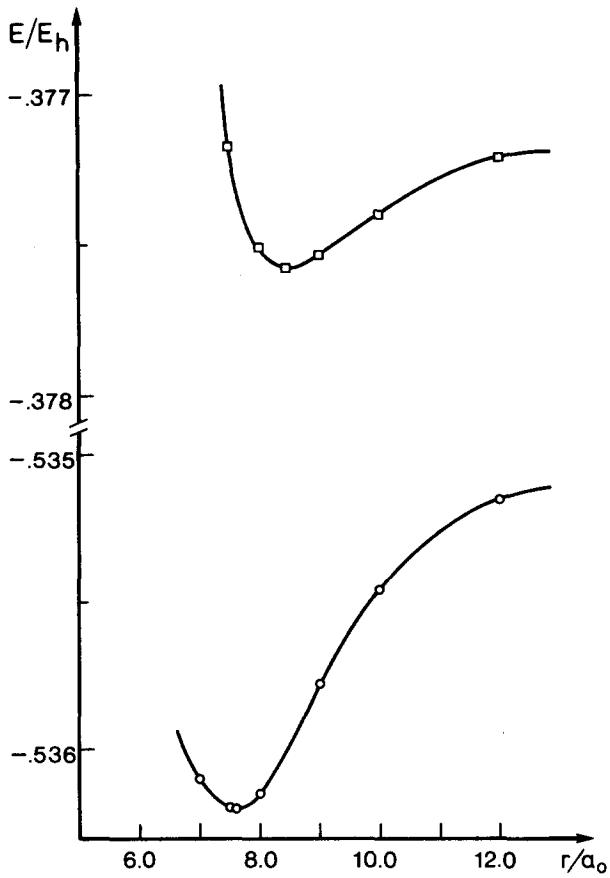

FIG. 2. Variational (upper part, □) and second-order corrected (lower part, ○) selected CI (NCF = 63) potential energy curves vs r(Cu–C), for the CuCO $^2\Sigma^+$ state, using the DZ basis set. The energies are relative to $-71.000\,00\,E_h$.

DZ + P basis set. It is well known[28] that calculations of this type are meaningful only if a large basis set is used, otherwise the actual interaction energy might be obscured by the basis set superposition error (BSSE).[29] The variational potential energy curves, both using the CAS space and a selected CI wave function at 5.0 a_0 with a number of configurations (NCF) of 64, are not bound. However, including the second-order perturbation correction, a minimun at 8.269 a_0 (see Fig. 3) is found. This trend is also maintained perturbing a single determinant wave function although the stabilization energy is somewhat weaker (see Fig. 4), reflecting the fact that well correlated wave functions are needed to obtain with confidence that part of the correlation energy responsible for the weak intermolecular interaction.

Table I summarizes the results obtained with the DZ and DZ + P basis sets. The energies are referred to E at 12 a_0 and represent a lower bound to the accurate interaction energy in each case. As Table I shows, the DZ + P ΔE best value represents a decrease of about $9\times10^{-4}E_h$ ($\sim$0.6 kcal/mol) with respect to the DZ result. In a recent study reported by Blomberg *et al.*[30,31] a similar trend was found for NiCO. Inclusion of d functions in the basis set for carbon and oxygen decreases the NiCO binding energy by 0.6 kcal/mol. However, in that case it was not important because of the larger interaction. The opposite situation occurs in the

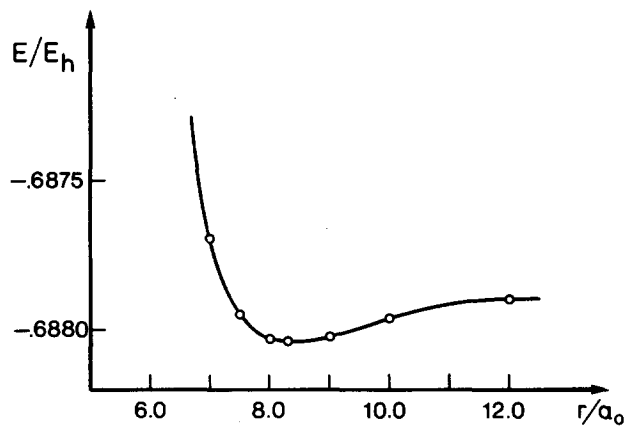

FIG. 3. Second-order corrected selected CI (NCF = 64) potential energy curve vs r (Cu–C) for the CuCO $^2\Sigma^+$ state using the DZ + P basis set. The energies are relative to $-71.000\,00\,E_h$.

CuCO bonding. However, further tests with a more flexible basis set are still desirable.

Another important factor to take into account is the variation of the C–O distance, so far kept fixed at the experimental value, 2.132 a_0. At r(Cu–C) = 7.5 a_0 where the complex is slightly bound using the DZ + P basis set, NCF = 64: $\Delta E_1 = E(7.5) - E(12.0) = -4.4\times10^{-5}\,E_h$; the optimal C–O distance is 2.185 a_0. An increase has taken place and the stabilization with respect to $(r_{\text{Cu-C}}, r_{\text{C-O}}) = (7.5, 2.132)$ is $\Delta E_{\text{opt1}} = E(7.5, 2.185) - E(7.5, 2.132) = -8.6\times10^{-4}E_h$. To elucidate how much of this stabilization energy comes from a weak Cu···CO interaction rather than the optimization of the C–O distance, this optimization has also been carried out at r(Cu–C) = 12.0 a_0. The optimal C–O distance was found at 2.171 a_0, being $\Delta E_{\text{opt2}} = E(7.5,\ 2.185) - E(12.0,\ 2.171) = \Delta E_1 - (\Delta E_{\text{opt1}} - \Delta E_{\text{opt2}}) = 4.3\times10^{-5}E_h$. If we assume that the energy retrieved from the C–O optimization at r(Cu–O) = 7.5 a_0 would be very similar to the one at $r_{\min}$(Cu–C) = 8.269 a_0, which is not unlikely, $\Delta E_{\text{opt}} = E(8.269) - E(12.0) \simeq E(8.269, 2.132) + \Delta E_{\text{opt1}} - \{E(12.0, 2.132) + \Delta E_{\text{opt2}}\} = -0.48\times10^{-4}E_h$. Thus, although the inter-

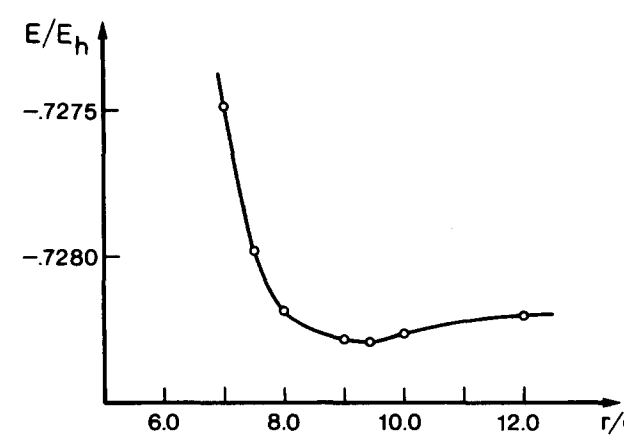

FIG. 4. Single configuration second-order corrected CI (NCF = 1) potential energy curve vs r(Cu–C) for the CuCO $^2\Sigma^+$ state using the DZ + P basis set. The energies are relative to $-71.000\,00\,E_h$.

Downloaded 29 Jan 2010 to 147.156.182.23. Redistribution subject to AIP license or copyright; see http://jcp.aip.org/jcp/copyright.jsp

TABLE I. Summary of the results obtained for the $CuCO\ ^2\Sigma^+$ ground state with the DZ and DZ + P basis sets (see Sec. II). ΔE is defined as the difference of $E(r_{min})$ and $E(12\ a_0)$; a negative ΔE indicates a stable, bound species.

		DZ		DZ + P	
CI space	Energy	r_{min}/a_0	$\Delta E\ 10^4/E_h$	r_{min}/a_0	$\Delta E\ 10^4/E_h$
CAS[a]	variational[b]	7.695	− 8.66	nonbound	
	total[c]	7.978	− 5.34	...	
Selected	variational[b]	8.461[d]	− 3.75[d]	nonbound[e,f]	
	total[c]	7.611[d]	− 10.42[d]	9.427[e]	− 0.93[e]
				8.269[f]	− 1.35[f]

[a] CAS-CI with seven active MOs (s_{Cu} and $\sigma,\pi,\sigma^*,\pi^*$ of CO), keeping $2e^-$ of opposite spins in each π subsystem and $3e^-$ in the σ active MOs (142 determinants, hence the two septuple excitations are discarded).
[b] From the variational part of the correlation energy.
[c] Including the 2nd order perturbation correction.
[d] Number of configurations (NCF) diagonalized is 63.
[e] NCF = 1
[f] NCF = 64

action at the minimun of the Cu–C distance has decreased by a factor of 3 with respect to the optimal C–O distance at r(Cu–C) = 12.0 a_0, the presence of a weak minimum is again evident and gives stronger support for the idea that a very shallow weak van der Waals minimum involving the $CuCO\ ^2\Sigma^+$ ground state is actually present.

The DZ + P basis set is not yet adequate enough to give quantitative results, but we think that it is good enough to ensure that a weak van der Waals complex is present in the range of 4.0 to 10.0 a_0 Cu–C distance, although it was not previously found.[6] The present results are also in agreement with the matrix isolation spectroscopy experiment of Kasai and Jones[9] although the influence of the matrix should be checked.

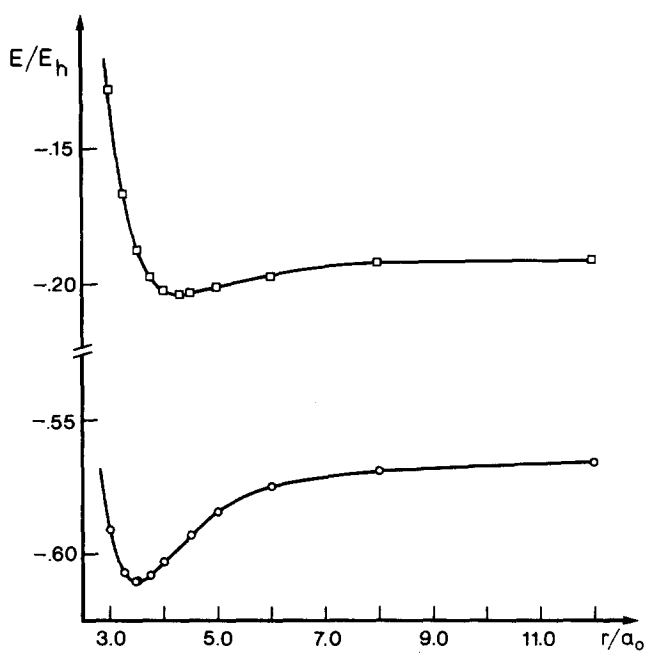

FIG. 5. Variational (upper part, □) and second-order corrected (lower part, ○) selected CI (NCF = 30) potential energy curves vs r(Cu–C) for the $CuCO\ ^2\Pi$ state, using the DZ + P basis set. The energies are relative to − 71.000 00 E_h.

B. CuCO $^2\Pi$ state

The MOs used for the CI calculations of the $CuCO\ ^2\Pi$ excited state were the localized MOs obtained for the CuCO ground state using the DZ + P basis set. Thus, the $^2\Pi$ state is described as a monoexcitation from the $4s^1$ to $4p_x^1$ (or $4p_y^1$). Although the MOs used are not optimal for this state, this procedure can be supported for the following reasons: both states involve a d^{10} closed shell for copper, so the main d electronic reorganization is taken into account, and the nature of the bonding in the $CuCO\ ^2\Pi$ state is more clearly noticed at CI level, as will be discussed in Sec. V.

The CI potential energy curves have been built using the reference space selected at the Cu–C distance of 4.0 a_0 with 30 determinants. We have studied the range between 3.0 and 12.0 a_0, keeping the C–O distance fixed at the experimental value. As Fig. 5 shows, when the second-order perturbation is included a pronounced well is obtained. With respect to the variational curve, the minimum is displaced towards a shorter Cu–C distances. Table II summarizes these results. Note how important it is to consider the second order perturbation correction in order to obtain adequate interaction energies. In this case, to consider $-\Delta E \simeq E_b$ (E_b = binding energy), will not involve a dramatic difference due to the strong bonding in the $^2\Pi$ state. In any case, we keep the ΔE notation which is more strictly correct.

IV. RESULTS FOR THE $CuCO^+$ COMPLEX

The $CuCO^+\ ^1\Sigma^+$ state may be described in terms of a carbonyl ligand, CO ($^1\Sigma^+$), and Cu^+ (d^{10}) metal atom. Thus, bonding in the $CuCO^+$ complex is expected to be quite strong due mainly to the electrostatic interaction and perhaps σ bonding and/or π backdonation.

In fact, as Fig. 6 shows, bonding in the $CuCO^+$ complex is present at the SCF and CI levels. The basis set employed is the DZ + P one. Recall that localization of the MOs before the CI step has been undertaken. A systematic study in the range of 3.0 to 12.0 a_0 was carried out, fixing the C–O distance equal to the experimental value. The 74 more important determinants selected at Cu–C distance of 4.0 a_0 have

Downloaded 29 Jan 2010 to 147.156.182.23. Redistribution subject to AIP license or copyright; see http://jcp.aip.org/jcp/copyright.jsp

TABLE II. Results obtained for the CuCO $^2\Pi$ state using the DZ + P basis set, including in the reference space the 30 more important determinants selected at r(Cu–C) = 4.0 a_0, keeping the C–O distance fixed at the experimental value. ΔE is defined as the difference of $E(r_{min})$ and $E(12\ a_0)$. A negative ΔE indicates a stable interaction.

CI energy	r_{min}/a_0	$E(12\ a_0)/E_h$	ΔE (eV)
Variational[a]	4.347	− 71.190 697	− 0.35
Total[b]	3.484	− 71.565 662	− 1.22

[a] From diagonalization of the reference space.
[b] Including the second-order perturbation correction.

TABLE III. Results obtained for the $(CuCO)^+$ $^1\Sigma^+$ state using the DZ + P basis set, including in the reference space the 74 more important determinants. ΔE is defined as the difference of $E(r_{min})$ and $E(12\ a_0)$. A negative ΔE indicates a stable interaction.

Energy	r_{min}/a_0	$E(12a_0)/E_h$	ΔE (eV)
SCF	4.067	− 70.935 982	− 0.75
CI variational[a]	4.556	− 71.219 316	− 0.44
CI total[b]	3.762	− 71.441 043	− 1.19

[a] From the variational part of the correlation energy.
[b] Including the second-order perturbation correction.

been used to build the CI potential energy curves.

Table III lists the r_{min} and ΔE values for the $CuCO^+$ complex. It can be noted how the variational part of the correlation energy increases the Cu–C optimal distance and diminishes ΔE, with respect to the SCF values. On the contrary, inclusion of the second-order perturbation correction works in the opposite way. As we will see in the forthcoming section, this behavior can be stated in a more general manner and has its cause in very subtle effects of the correlation energy.

Although $CuCO^+$ ($^1\Sigma^+$) and CuCO ($^2\Pi$) complexes have rather similar ΔE values, the optimal Cu–C distance is longer in the first case, so a different type of bonding is expected. In Cu–CO^+ the positive charge causes a strong electric field on CO and probably we are in a region where pure electrostatic interactions are dominant, mainly, charge–dipole and charge–induced dipole interactions. If the copper ion is replaced by a simple point charge, a computed ΔE value of − 0.93 eV is obtained. Thus, this simple model is quite reasonable and gives a picture of the nature of the Cu^+–CO interaction as will be established in the next section.

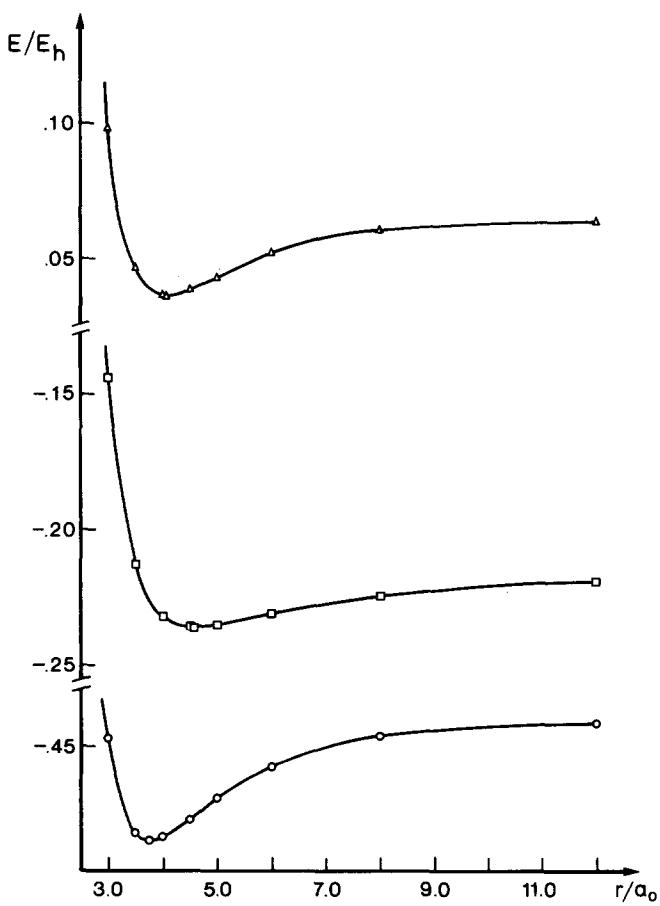

FIG. 6. From top to bottom: SCF potential energy curve (△) vs r(Cu–C) for the $CuCO^+$ ground state using the DZ + P basis set, and variational (□) and second-order corrected selected CI (○) (NCF = 74) potential energy curves. The energies are relative to − 71.000 00 E_h.

V. ANALYSIS AND DISCUSSION

The results reported in the previous sections show how much the interaction energy and the optimal metal–ligand distance is affected when electron correlation is taken into account and also the different behavior of the variational part of the correlation energy in relation to the total correlation energy, including the second-order perturbation corrections. Apart from the HF determinant, an important percentage in the CI wave function involves the intramolecular correlation of the CO molecule. Thus, in a first step, analysis of the main electronic correlation effects on the isolated CO molecule is drawn in order to be compared with the complexes considered. If we succeed in understanding how the CO molecule feels the presence of the Cu(^2S), Cu(^2P), and Cu^+(^1S) atoms, we would hopefully get some insight into the nature of the metal–carbon monoxide bonding.

As was stated earlier, localized MOs (LMOs) are used in all cases. Thus, in order to see how suitable are these MOs for CI purposes, and using the DZ + P basis set, an iterative selection has been performed with both the LMOs and CMOs for sake of comparison. As can be seen from Fig. 7, the number of determinants necessary to obtain a variational correlation energy of − 0.129 E_h decreases from ~100 (CMOs) to 65 (LMOs), in agreement with previous CAS-CI analyses[21] of the CO molecule at the DZ level. It is also noticed that the dispersion of the second-order corrected correlation energies results is smaller than the variational results giving an estimation of the accuracy of a second-order multireference perturbative algorithm like CIPSI.

Table IV shows the more important contributions in decreasing order in the CI wave function using LMOs and also the corresponding coefficients with CMOs, both of similar quality, i.e., they pick up nearly the same variational correlation energy. Most of the contributions have a larger weight when using LMOs than with CMOs, since in this procedure the maximization of the virtual–occupied ex-

Downloaded 29 Jan 2010 to 147.156.182.23. Redistribution subject to AIP license or copyright; see http://jcp.aip.org/jcp/copyright.jsp

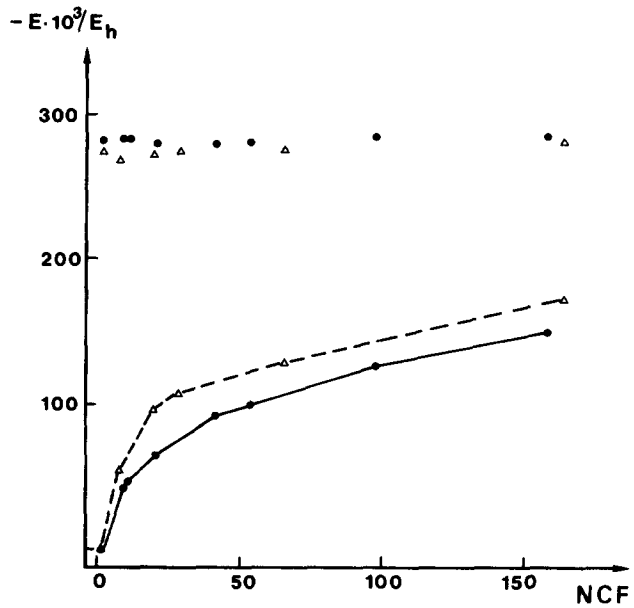

FIG. 7. Variational (lower part) and second-order corrected (upper part) correlation energies of the CO molecule as function of the number of determinants in the variational wave function (NCF) (CIPSI algorithm). ●—● canonical MOs. Δ- - -Δ occupied and virtual MOs from the HAO procedure.

change interaction is implicitly involved. The transformed virtual orbitals are especially suited to describe the $(i)^2 \rightarrow (i^*)^2$, and introduce important interactions between the ground state configuration and the excited ones of the type $(ij) \rightarrow (i^*j^*)$. The more important contributions account for the nondynamical correlation of the CO bond. Also, it is interesting to recall that *a priori* in the valence

TABLE IV. Using the DZ + P basis set, the more important contributions, by spin or symmetry constraints, to the multideterminantal CI wave function $\Psi = C_0\Phi_0 + \Sigma_{J=I}^{NCF} C_J\Phi_J$ for CO, employing localized molecular orbitals (LMOs), are listed. The corresponding coefficients obtained with canonical molecular orbitals (CMOs) are also shown. Only one of an equivalent set of configurations is shown.

		C_J	
J	Φ_J[a]	LMOs (NCF = 65)	CMOs (NCF = 97)
0	Φ_0[b]	0.969	0.969
I	$(\pi_x)^2 \rightarrow (\pi_x^*)^2$	− 0.089	− 0.072
II	$\pi_x\bar{\pi}_y \rightarrow \pi_x^*\bar{\pi}_y^*$	− 0.065	− 0.050
III	$(n_C)^2 \rightarrow (\pi_x^*)^2$	− 0.059	− 0.062
IV	$(\sigma)^2 \rightarrow (\sigma^*)^2$	− 0.046	c
V	$\pi_x\pi_y \rightarrow \pi_x^*\pi_y^*$	− 0.046	− 0.034
VI	$(n_C)^2 \rightarrow (n_C^*)^2$	− 0.041	− 0.044
VII	$\sigma\bar{\pi}_x \rightarrow \sigma^*\bar{\pi}_x^*$	0.038	c
VIII	$\pi_x \rightarrow \pi_x^*$	− 0.029	− 0.025
.	.	.	.
.	.	.	.

[a] Refers to the ground state determinant.
[b] Represents the ground state determinant: $|n_C^2 n_O^2 \sigma^2 \pi_x^2 \pi_y^2|$
[c] Not present (see the text).

CAS-CI, excitations of type III $(n_c)^2 \rightarrow (\pi_x^*)^2$, or VI $(n_C)^2 \rightarrow (n_C^*)^2$, associated with delocalization and radial correlation of the carbon lone pair, respectively, would not be included. These lead to strong perturbations, a point of reflection when the CAS approach is chosen and the dynamical correlation energy is calculated by perturbative methods.

Monoexcitations $\pi_x \rightarrow \pi_x^*$, $\bar{\pi}_x \rightarrow \bar{\pi}_x^*$ (and the corresponding y contributions), type VIII, can be related to the

TABLE V. Using the DZ + P basis set, the more important contributions to the multideterminantal CI wave function $\Psi = C_0\Phi_0 + \Sigma_{J=I}^{NCF} C_J\Phi_J$, being NCF = 64, for the $CuCO\ ^2\Sigma^+$ state, employing LMOs, are shown for various r(Cu–C) distances. The C–O distance is kept fixed at the experimental value. Only one of an equivalent set of configurations is shown.

		C_J		
J	Φ_J	$r = 7.0\ a_0$	$r = 8.269\ a_0$	$r = 10.0\ a_0$
0	$\Phi_0 = \|\{CO\}\{d_{Cu}^{10}\}\bar{s}_{Cu}\|$	0.963	0.963	0.963
Intramolecular correlation of CO				
I	$(\pi_x)^2 \rightarrow (\pi_x^*)^2$	− 0.077	− 0.077	− 0.077
II	$\pi_x\bar{\pi}_y \rightarrow \pi_x^*\bar{\pi}_y^*$	− 0.056	− 0.056	− 0.056
III	$(n_C)^2 \rightarrow (\pi_x^*)^2$	− 0.056	− 0.056	− 0.056
IV	$(\sigma)^2 \rightarrow (\sigma^*)^2$	− 0.044	− 0.044	− 0.044
V	$\pi_x\pi_y \rightarrow \pi_x^*\pi_y^*$	− 0.040	− 0.040	− 0.040
VI	$(n_C)^2 \rightarrow (n_C^*)^2$	− 0.038	− 0.039	− 0.039
VII	$\sigma\bar{\pi}_x \rightarrow \sigma^*\bar{\pi}_x^*$	0.036	0.036	0.036
VIII	$\pi_x \rightarrow \pi_x^*$	− 0.019	− 0.020	− 0.020
	$\bar{\pi}_x \rightarrow \bar{\pi}_x^*$	− 0.020	− 0.020	− 0.020
.	.	.	.	.
.	.	.	.	.
Intraatomic correlation of CU				
IX	$\bar{s} \rightarrow \bar{s}^*$	0.049	0.049	0.050
X	$(d_\pi)^2 \rightarrow (d_\pi^*)^2$	− 0.037	− 0.037	− 0.037
XI	$(d_\delta)^2 \rightarrow (d_\delta^*)^2$	− 0.037	− 0.037	− 0.037
XII	$(d_\sigma)^2 \rightarrow (d_\sigma^*)^2$	− 0.034	− 0.035	− 0.035
.	.	.	.	.
.	.	.	.	.

Downloaded 29 Jan 2010 to 147.156.182.23. Redistribution subject to AIP license or copyright; see http://jcp.aip.org/jcp/copyright.jsp

well known fact that for reproducing the experimental sign of the CO dipole moment (C^-O^+), monoexcitations are needed.[32] Indeed, it has been found[33] that the Hartree–Fock approximation overestimates the ionic structures which follow the electronegativity difference and the main work by correlation is the increase of the neutral components; the polarity appears through the unequal coefficients of the monoionic situations.

In the first order correlated wave function for the CuCO $^2\Sigma^+$ state it is found that the HF determinant has the more important contribution (92.7%), the remaining is due to the intramolecular correlation of CO (4.4%), and to the intraatomic correlation of the copper atom (2.9%). Table V shows the main coefficients at several r(Cu–C) distances. It is noted that from 7.0 to 10.0 a_0, the intra-CO and Cu correlation keeps quite constant. For the CO fragment, the numbering of the type of contributions is associated to that corresponding to the isolated CO (Table IV) all having the same behavior, and implying the same physical meaning as discussed above. The main contributions to the intraatomic correlation of the copper atom ($\bar{s}\rightarrow\bar{s}^*$) tends to enlarge the two inner Gaussian coefficients and to reduce the outer one

TABLE VI. Using the DZ + P basis set, the more important contributions to the multideterminantal CI wave function $\Psi = C_0\Phi_0 + \Sigma_{J=1}^{NCF} C_J\Phi_J$ (NCF = 30), for the CuCO $^2\Pi$ state, employing the LMOs of the CuCO $^2\Sigma^+$ state are listed for several r(Cu–C) distances.

		C_J		
J	Φ_J	$r = 3.0\,a_0$	$r = 3.484\,a_0$	$r = 6.0\,a_0$
0	$\Phi_0 = \lvert\{CO\}\{d_{Cu}^{10}\}\bar{p}_{x\,Cu}\rvert$	0.894	0.918	0.953
Intramolecular correlation of CO				
I	$(\pi_x)^2\rightarrow(\pi_x^*)^2$	−0.087	−0.090	−0.090
	$(\pi_y)^2\rightarrow(\pi_y^*)^2$	−0.087	−0.090	−0.090
II	$\pi_x\bar{\pi}_y\rightarrow\pi_x^*\bar{\pi}_y^*$	−0.062	−0.064	−0.064
	$\bar{\pi}_x\pi_y\rightarrow\bar{\pi}_x^*\pi_y^*$	−0.062	−0.064	−0.064
III	$(n_C)^2\rightarrow(\pi_x^*)^2$	−0.034	−0.036	−0.045
	$(n_C)^2\rightarrow(\pi_y^*)^2$	−0.034	−0.036	−0.045
IV	$(\sigma)^2\rightarrow(\sigma^*)^2$	−0.044	−0.045	−0.048
V	$\pi_x\pi_y\rightarrow\pi_x^*\pi_y^*$	−0.041	−0.042	−0.043
	$\bar{\pi}_x\bar{\pi}_y\rightarrow\bar{\pi}_x^*\bar{\pi}_y^*$	−0.041	−0.042	−0.043
VI	$(n_C)^2\rightarrow(n_C^*)^2$	−0.028	−0.033	−0.040
VII	$\sigma\bar{\pi}_x\rightarrow\sigma^*\bar{\pi}_x^*$	0.038	0.040	0.041
	$\bar{\sigma}\pi_x\rightarrow\bar{\sigma}^*\pi_x^*$	0.038	0.040	0.041
	$\sigma\bar{\pi}_y\rightarrow\sigma^*\bar{\pi}_y^*$	0.038	0.040	0.041
	$\bar{\sigma}\pi_y\rightarrow\bar{\sigma}^*\pi_y^*$	0.038	0.040	0.041
VIII	$\pi_x\rightarrow\pi_x^*$	−0.034	−0.033	−0.031
	$\bar{\pi}_x\rightarrow\bar{\pi}_x^*$	−0.033	−0.033	−0.031
	$\pi_y\rightarrow\pi_y^*$	−0.034	−0.034	−0.031
	$\bar{\pi}_y\rightarrow\bar{\pi}_y^*$	−0.034	−0.034	−0.031
Intraatomic correlation of Cu				
IX	$\bar{p}_x\rightarrow\bar{p}_x^*$	0.114	0.090	0.115
X	$(d_\delta)^2\rightarrow(d_\delta^*)^2$	−0.040	−0.042	−0.045
.	.	.	.	.
.	.	.	.	.
Charge transfer from Cu to CO				
XI	$\bar{p}_{x\,Cu}\rightarrow\bar{\pi}_{x\,C}^*$	0.275	0.237	0.121
XII	$\bar{p}_{x\,Cu}\rightarrow\bar{\pi}_x^*$	−0.220	−0.172	−0.058
XIII	$\bar{p}_{x\,Cu}\rightarrow\bar{\pi}_{x\,O}^*$	−0.112	−0.096	−0.046

TABLE VII. Net atomic charges and total overlap population of CO ground state and $CuCO^+$ complex, for various r(Cu–C) distances.

		r(Cu–C)/a_0		
Atoms	CO	3.500	4.067	5.000
C	0.066	0.061	0.078	0.062
O	−0.066	0.070	0.058	0.027
Cu		0.867	0.866	0.917
C–O	0.671	0.779	0.775	0.756
Cu–C		0.141	0.099	0.050

which represents the copper s shell (recall that a triple-zeta s basis set is used), and can be ascribed to the spurious term of autorepulsion of the Nesbet operator.[23] The other contributions take into account the d shell radial correlation of the copper atom.

A quite different situation is found for the CuCO $^2\Pi$ state. At r(Cu–C) = 3.484 a_0, the HF determinant accounts for 84.2% of the CI wave function, intramolecular of CO 4.4%, intraatomic correlation of the copper atom 1.9%, and the contributions responsible for the charge transfer from the copper atom to CO 9.5%. Table VI shows the presence of a slight π^- and spin polarization in this case due to the beta electron placed on the p_x copper atomic orbital, mainly through the monoexcitations of the π system. The intraatomic correlation of copper involves the radial correlation of the d shell and the p adaptation. The highest weight of the charge transfer from copper to CO implies the second virtual MO, $\pi_{x_C}^*$, which is polarized toward the carbon atom; contributions XII and XIII implying the valence π_x^* and the third π virtual, $\pi_{x_O}^*$ MO, which is polarized towards the oxygen atom, are also important.

Stabilization is found at both SCF and CI levels for the interaction of the $Cu^+(^1S)$ metal atom with the $CO(^1\Sigma^+)$ ligand. To a first approximation, the SCF level should be adequate to describe the major effects in these types of electrostatic interaction. In order to understand better the bonding at the SCF level, Table VII shows net atomic charges and total overlap populations, from Mulliken population analysis, for the $CuCO^+$ complex at several Cu–C distances and also for the free CO, for sake of comparison. Charge transfer from CO to the copper monoion seems to take place. The Cu–C overlap population diminishes when the Cu–C distance increases. However, at the optimal SCF Cu–C distance, 4.067 a_0, the positive net atomic charge on the carbon atom is largest and also charge transfer to the copper atom becomes more favorable. The total population of atomic valence orbitals indicates (Table VIII) that the orbitals involved in the metal–ligand bonding are the carbon lone pair (notice the s, p_z orbital reorganization in the complex with respect to the isolated CO) and the s, p_z atomic orbitals of the copper monoion (notice that the role of the p_z orbital is important). On the other hand, if π backbonding would be present, a decreasing of the d_π population (d_{xz} and d_{yz} orbitals) might be expected. That is not the case and π backbonding is negligible, which is appearing to be a characteristic find in the copper–monoion–ligand interactions.[34] Nevertheless, a more pronounced population diminution

Downloaded 29 Jan 2010 to 147.156.182.23. Redistribution subject to AIP license or copyright; see http://jcp.aip.org/jcp/copyright.jsp

TABLE VIII. Total population of atomic valence orbitals of CO ground state and $CuCO^+$ complex, at different r(Cu–C) distances.

		r(Cu–C)/a_0		
Orbital	CO	3.500	4.067	5.000
C(s)	1.840	1.556	1.594	1.666
C(p_x)	0.474	0.556	0.541	0.524
C(p_y)	0.474	0.556	0.541	0.524
C(p_z)	1.040	1.165	1.146	1.124
C($d_{x^2-y^2}$)	0.000	0.000	0.000	0.000
C(d_{z^2})	0.032	0.028	0.028	0.028
C(d_{xy})	0.000	0.000	0.000	0.000
C(d_{xz})	0.037	0.039	0.036	0.036
C(d_{yz})	0.037	0.039	0.036	0.036
O(s)	1.708	1.735	1.732	1.731
O(p_x)	1.482	1.409	1.415	1.430
O(p_y)	1.482	1.409	1.415	1.430
O(p_z)	1.370	1.350	1.353	1.356
O($d_{x^2-y^2}$)	0.000	0.000	0.000	0.000
O(d_{z^2})	0.010	0.011	0.011	0.010
O(d_{xy})	0.000	0.000	0.000	0.000
O(d_{xz})	0.007	0.008	0.008	0.008
O(d_{yz})	0.007	0.008	0.008	0.008
Cu(s)		0.127	0.090	0.045
Cu(p_x)		0.001	0.000	0.000
Cu(p_y)		0.001	0.000	0.000
Cu(p_z)		0.064	0.057	0.038
Cu($d_{x^2-y^2}$)		2.000	2.000	2.000
Cu(d_{z^2})		1.964	1.989	2.000
Cu(d_{xy})		2.000	2.000	2.000
Cu(d_{xz})		1.988	1.999	2.000
Cu(d_{yz})		1.988	1.999	2.000

from 2.0 is found for the d_{z^2} atomic orbital of copper which enable us to wonder whether s, d_{z^2} or s, p_z, d_{z^2} copper hybridization is taking place.

In order to avoid the arbitrary division of overlap population used in a Mulliken population analysis, especially regarding metallic complexes,[35–37] the corresponding orbital transformation[36(a),38] has been carried out. In the corresponding orbital analysis, the $1-\lambda_i$ values give a quantitative measure of the extent of the change due to the interaction between the two fragments A and B of a complex AB. The λ_i are obtained from the diagonalization of the $SS^\dagger$, S being the overlap matrix of the orbitals of a fragment and those of the complex.

The highest $(1-\lambda)$ values of the smallest nonzero λ's for $CuCO^+$ are given in Table IX; the remaining larger λ's are all essentially 1. If we consider the corresponding eigenvalue between the CO and $CuCO^+$ occupied orbitals the $(1-\lambda)$ values show a very small change of the CO orbitals, and seems to be slightly more pronounced at the SCF minimum. The corresponding orbitals associated with this λ, ϕ'_m for CO and Ψ'_m for $CuCO^+$ ($m=5$) are mainly representing the carbon lone pair, and in Ψ'_m the participation of the s atomic orbital of copper is also noted with some p_z hybridization, and polarization towards the carbon atom. Even if there is some charge donation $n_C \rightarrow s_{Cu}$, the corresponding $(1-\lambda)$ value demonstrates that there is very little CO σ to metal donation. In fact, if we estimate the donation by assuming that the deviation from 1 is due entirely to such CO σ to metal donation, at the optimal SCF Cu–C distance it is only 0.02 electrons, $0.02 = 2(1-\lambda)$.

TABLE IX. The highest $(1-\lambda)$ values of the smallest nonzero corresponding orbital eigenvalues, λ, see Eq. (4), related with CO and $CuCO^+$ (a), and Cu^+ and $CuCO^+$ (b) occupied orbitals, at different Cu–C distances.

	$(1-\lambda)\times 10^2$		
	3.500 a_0	4.067 a_0	5.000 a_0
(a) $n_C \rightarrow s_{Cu}$	1.132	1.134	0.928
(b) Cu(d_{z^2})	1.044	0.450	0.073
Cu(d_π)	0.367	0.070	0.018

The corresponding orbitals between the metal and $CuCO^+$ are consistent with the results from Mulliken population analysis. The smallest λ for the Cu^+–$CuCO^+$ corresponding orbitals is associated with the d_{z^2} orbital of copper, showing some hybridization with the s atomic orbital (the role of the p_z orbital is less important) which diminishes going to longer Cu–C distances. Table IX also shows the penultimate $(1-\lambda)$ value for the metal–complex corresponding analysis which is associated to the d_π orbital. It could be related to the π backdonation, appearing to be negligible (10^{-3} electrons at the SCF minimum).

Let us now consider the main features of the $CuCO^+$ CI corrections. In the first-order correlated wave function at r(Cu–C) = 3.762 a_0, the HF determinant has a weight of 92.9%, intramolecular correlation of CO 4.7%, intraatomic correlation of the copper atom 2.3%, and the polarization,

TABLE X. Using the DZ + P basis set the more important contributions to the CI wave function $\Psi = C_0\Phi_0 + \Sigma_{J=I}^{NCF} C_J\Phi_J$ (NCF = 74) for the ground state of the $CuCO^+$ molecule are shown. LMOs are used; r refers to the Cu–C separation.

		C_J		
J	Φ_J	$r=3.0\,a_0$	$r=3.762\,a_0$	$r=6.0\,a_0$
0	$\Phi_0\|\{CO\}\{d^{10}\}\|$	0.966	0.964	0.963
Intramolecular correlation of CO				
I	$(\pi_x)^2 \rightarrow (\pi_x^*)^2$	−0.090	−0.089	−0.083
II	$\pi_x\bar{\pi}_y \rightarrow \pi_x^*\bar{\pi}_y^*$	−0.064	−0.063	−0.060
III	$(n_C)^2 \rightarrow (\pi_x^*)^2$	−0.042	−0.045	−0.051
IV	$(\sigma)^2 \rightarrow (\sigma^*)^2$	−0.044	−0.044	−0.044
V	$\pi_x\pi_y \rightarrow \pi_x^*\pi_y^*$	−0.044	−0.044	−0.042
VI	$(n_C)^2 \rightarrow (n_C^*)^2$	−0.022	−0.029	−0.039
VII	$\sigma\bar{\pi}_x \rightarrow \sigma^*\bar{\pi}_x^*$	0.038	0.037	0.037
VIII	$\pi_x \rightarrow \pi_x^*$	−0.021	−0.020	−0.019
.	.	.	.	.
.	.	.	.	.
Intraatomic correlation of Cu				
IX	$(d_\delta)^2 \rightarrow (d_\delta^*)^2$	−0.035	−0.035	−0.035
X	$(d_\pi)^2 \rightarrow (d_\pi^*)^2$	−0.026	−0.031	−0.033
.	.	.	.	.
.	.	.	.	.
Charge transfer from CO to Cu				
XI	$n_C\bar{n}_C \rightarrow s_{Cu}\bar{n}_C^*$	−0.018	−0.020	−0.014

Downloaded 29 Jan 2010 to 147.156.182.23. Redistribution subject to AIP license or copyright; see http://jcp.aip.org/jcp/copyright.jsp

and charge transfer from CO to Cu about 0.1%. Table X shows that the behavior of the intra-CO correlation is essentially the same as for free CO. Notice how the σ system is quite unperturbed by the presence of the Cu^+ atom. However, the π system feels the metal more. For instance, type I contribution, which merely increases the weight of the neutral situations and diminishes the ionic ones for the π system, the weight (square of the coefficient) tends to smaller values when lengthening the Cu–C distance. This implies that the ionic situations are penalized at shorter distances. On the other hand, delocalization of the carbon lone pair and the carbon radial correlation becomes more effective at longer distances. The intraatomic correlation of Cu involves the radial correlation of d shell, for the d_δ is constant but for the d_π the weight increases when increasing the Cu–C separation. Charge transfer from CO to Cu, and polarization, present a larger contribution at $r(\text{Cu–C}) = 3.762\ a_0$. Among the more important contributions taken into account by the second order perturbation correction has also been noted the diexcitation $n_C^2 \rightarrow s_{Cu}^2$ which properly accounts for the expected charge transfer from CO to copper. Thus, with the enlargement of the reference space that type of contribution would be treated variationally. However, this point does not hold for any type of excitation representing π-backbonding, which means that even using reasonable larger reference spaces, π backdonation could be treated perturbatively.

We can now explain the displacements of the optimal Cu–C distance (see Fig. 6) at the CI level with respect to the SCF approach, which can be seen as a general trend as far as our own experience is concerned. As has been shown, the intramolecular correlation of the ligand plays an important role in the first-order correlated wave function of the complex. The main effects of the intramolecular correlation of CO can be related to the left–right correlation of the C–O bond, implying a decreasing of certain highly unfavorable ionic situations and increasing the weight of the neutral ones, thus, it is not surprising to obtain a longer optimal distance (or a decrease of the stabilization energy). Now, all the many small contributions taken by perturbation technique, as a whole, are quite relevant and end up giving, even more pronounced, the SCF behavior shorter optimal distance (or a higher stabilization energy).

In the last few years great efforts have been devoted in order to understand the metal–CO bond in terms of σ and/or π bonding, since it is an extremely useful concept to rationalize this important type of bonding. The constrained space orbital variation (CSOV) technique[36(b)] has been successfully applied, at SCF and CASSCF levels, as a method for decomposing the bonding into intermolecular donations and intramolecular polarizations. From various studies concerning the interaction of CO with transition metals[8] as well as for *sp* metals,[36] the net bonding of CO to the metal has been described as the result of the sum of the σ repulsion and the π bonding. The total bond becomes weaker as the number of metal σ electrons is increased, i.e., as the σ repulsion increases. In general, little σ donation charge transfer from CO to the metal has been found which can be attributed [36(a)] to the relatively high ionization potential of CO. Similar conclusions[39] are obtained from analysis of the dipole moment and the electrons distributions determined from a variational CI wave function. Thus, the metal–CO bonding can be characterized primarily as a π donation from metal to CO π^* and if there are metal σ electrons, σ polarization takes place in order to reduce the repulsion in this space.

The present work shows that the $^2\Pi$ state of CuCO exhibits a pronounced minimum in its potential energy curve. On the contrary, the $^2\Sigma^+$ of CuCO has a weakly bound potential curve. These findings are in agreement with the regularities noted for metal–CO systems.[36(a),39–41] In fact, the CuCO $^2\Pi$ state with no metal σ electrons is strongly stabilized realtive to the interaction of $Cu(^2P)$ and $CO(^1\Sigma^+)$ at 12.0 a_0 although it does not compensate the energy difference between the $Cu(^2P)$ and $Cu(^2S)$ and the weakly bound $^2\Sigma^+$ state, with one metal σ electron, becomes the ground state as it has been previously reported.[5] On the other hand, although the interaction energies for CuCO $^2\Pi$ and $CuCO^+$ $^1\Sigma^+$ states are similar, the type of bonding is quite different π bonding and electrostatic nature, respectively.

We can also compare the CuCO $^2\Sigma^+$ and $CuCO^+$ $^1\Sigma^+$ states with the results recently reported for the NiCO $^1\Sigma^+$ and $NiCO^+$ $^2\Sigma^+$ states. These latter two present a total D_e very similar, ~ 1.2 eV,[8,31] meanwhile the bonding is very different in character: π bonding for the neutral, and due to the attraction of the ligand lone pair by the positive charge, along with charge–dipole electrostatic interaction for the ionic form. Thus, for the metal–CO ions the electrostatic attraction seems to play the more important role, and not the number of metal σ or π electrons, since for the $CuCO^+$ $^1\Sigma^+$ and $NiCO^+$ $^2\Sigma^+$ the stabilization energies are of the same order. However, for the neutral complexes the number of metal σ electrons is crucial. Thus, since the *s* promotion to the *d* filled shell of Cu is not feasible for the CuCO $^2\Sigma^+$ state, as in NiCO $^1\Sigma^+$, only a weak van der Waals interaction is found. Also, it can be noticed that the isoelectronic $NiCO(^1\Sigma^+)$ and $CuCO^+(^1\Sigma^+)$ complexes have a similar interaction energies but rather different bonding character.

VI. SUMMARY

The use of occupied and virtual localized MOs, with an optimal space of valence virtual MOs, is proven to be an advantageous and suitable way to build reliable potential energy curves since the same basic type of correlation is kept and therefore the same physical meaning holds at all distances. Moreover, the present protocol allows us to look at the major effects which involve the variational and also perturbational part of correlation energy. The importance of picking up the many thousands of minor contributions, as a whole, in order to obtain a correct description of the bonding has been stressed.

There is some theoretical support for a very weak van der Waals interaction energy for the CuCO $^2\Sigma^+$ state. A completely quantitative evaluation of this interaction should take into account the influence on the results of: (i) very large "adequate" basis sets, (ii) geometry optimization, and (iii) type of CI employed: highly correlated wave functions would be desirable.

Although very similar interaction energies are obtained for the CuCO $^2\Pi$ and $CuCO^+$ $^1\Sigma^+$ states, the driving forces

Downloaded 29 Jan 2010 to 147.156.182.23. Redistribution subject to AIP license or copyright; see http://jcp.aip.org/jcp/copyright.jsp

for bonding are quite different. Due to the special choice of the MOs used for the CI calculation of the CuCO $^2\Pi$ states it is clearly seen that the p_π donation plays a fundamental role. Moreover, no d_π backbonding excitations are present either in the variational wave function or among the more important ones included by perturbation theory. On the contrary, for the $CuCO^+$ $^1\Sigma^+$ complex the main interaction is of an electrostatic nature; from the Mulliken population analysis and also using the corresponding orbital transformation analysis, it is concluded that the π backdonation is negligible and although certain σ charge transfer occurs, it is not important.

The present findings are consistent with the previously accepted idea of the neutal metal–CO bonding as a balance of σ repulsion and π backdonation. However, for the ionic metal–CO bonding the pure electrostatic interactions seem to play a fundamental role.

ACKNOWLEDGMENTS

It is with great pleasure that we express our gratitude to Dr. J. P. Malrieu for his constant interest and helpful advice. We are also grateful to Dr. M. Pélissier and Dr. F. Illas for helpful discussions and technical assistance. We wish to acknowledge the group of the Laboratoire de Physique Quantique of Toulouse (France) for providing us with the PSHONDO and CIPSI programs and kindly sharing computer time, allowing us to perform part of the calculations reported here. The present work has been supported by the CAICYT Project No. 714/84. One of us (M. M.) acknowledges a fellowship from the Generalitat Valenciana.

[1] M. L. Poutsma, L. F. Elek, P. A. Ibarbia, A. P. Risch, and J. A. Rabo, J. Catal. **52**, 157 (1978).
[2] P. Sabatier and J. B. Senderens, J. Chem. Soc. **88**, 333 (1905).
[3] F. Fischer and H. Tropsch, Brennst. Chem. **7**, 97 (1926); Chem. Ber. **59**, 830 (1926).
[4] (a) J. T. Kummer, T. W. Dewitt, and P. H. Emmett, J. Am. Chem. Soc. **70**, 3632 (1948); (b) G. Henrici-Olivé and S. Olivé, Angew. Chem. Int. Ed. Engl. **15**, 136 (1976); (c) E. L. Muetterties and J. Stein, Chem. Rev. **79**, 479 (1979); (d) C. K. Rofer-de Poorter, Chem. Rev. **81**, 447 (1981); (e) A. Deluzarche, J. P. Hindermann, R. Kieffer, J. Cressely, and A. Kiennemann, Bull. Soc. Chim. Fr. II-329 (1982); (f) M. Boudart and M. A. McDonald, J. Phys. Chem. **88**, 2185 (1984); (g) W. A. Goddard III, S. P. Walch, A. K. Rappé, T. H. Upton, and C. F. Melius, J. Vac. Sci. Technol. **14**, 416 (1977); (h) I. G. Csizmadia, *Quantum Theory of Chemicals Reactions*, edited by R. Daudel, A. Pullman, L. Salem, and A. Veillard (Reidel, Dordrecht, 1982), Vol. III, pp. 77–84; (i) G. Henrici-Olivé and S. Olivé, J. Mol. Catal. **17**, 89 (1982); (j) J. Phys. Chem. **88**, 2426 (1984).
[5] P. S. Bagus, K. Hermann, and M. Seel, J. Vac. Sci. Technol. **18**, 435 (1981).
[6] T. -K. Ha and M. T. Nguyen, J. Mol. Struct. Theochem. **109**, 331 (1984).
[7] P. S. Bagus, C. J. Nelin, and C. W. Bauschlicher Jr., J. Vac. Sci. Technol. A **2**, 905 (1984).
[8] C. W. Bauschlicher Jr., J. Chem. Phys. **84**, 260 (1986); on CuH_2O see also, J. Sauer, H. Haberlandt, and G. Pacchioni, J. Phys. Chem. **90**, 3051 (1986).
[9] P. H. Kasai and P. M. Jones, J. Am. Chem. Soc. **107**, 813 (1985).
[10] H. Huber, E. P. Kündig, M. Moskovits, and G. A. Ozin, J. Am. Chem. Soc. **97**, 2097 (1975).
[11] J. A. Howard, B. Mile, J. R. Morton, K. F. Preston, and R. Sutcliffe, J. Phys. Chem. **90**, 1033 (1986).
[12] J. P. Daudey (private communication).
[13] M. Dupuis, J. Rys, and H. F. King, J. Chem. Phys. **65**, 111 (1976).
[14] Ph. Durand and J. C. Barthelat, Theor. Chim. Acta. **38**, 283 (1975).
[15] J. C. Barthelat and Ph. Durand, Gazz. Chim. Ital. **108**, 225 (1978).
[16] J. P. Daudey, J. C. Barthelat, and Ph. Durand, *Molecular ab initio Calculations Using Pseudopotentials*, Technical Report (Laboratoire de Physique Quantique, Toulouse, 1981).
[17] M. Pélissier, J. Chem. Phys. **75**, 775 (1981).
[18] G. Trinquier, J. C. Barthelat, and J. Satge, J. Am. Chem. Soc. **104**, 5931 (1982).
[19] See, e.g., V. McKoy and O. Sinanoglu, *Modern Quantum Chemistry*, edited by O. Sinanoglu (Academic, New York, 1965), Vol. 2, pp. 23–32.
[20] (a) P. E. M. Siegbahn, A. Heiberg, B. O. Roos, and B. Levy, Phys. Scr. **21**, 323 (1980); (b) B. O. Roos, P. R. Taylor, and P. E. M. Siegbahn, Chem. Phys. **48**, 157 (1980).
[21] F. Illas, M. Merchán, M. Pélissier, and J. P. Malrieu, Chem. Phys. **107**, 361 (1986).
[22] G. Chambaud, M. Gérard-Ain, E. Kassab, B. Levy, and P. Pernot, Chem. Phys. **90**, 271 (1984).
[23] R. K. Nesbet, Rev. Mod. Phys. **35**, 552 (1963).
[24] B. Huron, J. P. Malrieu, and P. Rancurel, J. Chem. Phys. **58**, 5745 (1973).
[25] (a) P. S. Epstein, Phys. Rev. **28**, 690 (1926); (b) R. K. Nesbet, Proc. R. Soc. London Ser. A **230**, 312, 922 (1955).
[26] (a) C. Moller and M. S. Plesset, Phys. Rev. **46**, 618 (1934); (b) J. P. Daudey and J. P. Malrieu, *Studies in Physical and Theoretical Chemistry*, edited by R. Carbó (Elsevier, Amsterdam, 1982), Vol 21, pp. 35–64.
[27] G. Herzberg, *Spectra of Diatomic Molecules* (Van Nostrand, New York, 1950).
[28] See, e.g., P. Cársky and M. Urban, *Lecture Notes in Chemistry: Ab Initio Calculations, No. 16* (Springer, Berlin, 1980).
[29] (a) N. R. Kestner, J. Chem. Phys. **48**, 252 (1968); (b) S. F. Boys and F. Bernardi, Mol. Phys. **19**, 553 (1970); (c) J. P. Daudey, P. Claverie, and J. P. Malrieu, Int. J. Quantum Chem. **23**, 1 (1974); (d) N. S. Ostlund and D. L. Merrifield, Chem. Phys. Lett. **39**, 612 (1976); (e) S. L. Price and A. J. Stone, Chem. Phys. Lett. **65**, 127 (1979); (f) W. A. Sokalski, S. Roszak, P. C. Hariharan, and J. J. Kaufman, Int. J. Quantum Chem. **23**, 847 (1983); (g) F. G. Olivares del Valle, S. Tolosa, J. J. Esperilla, E. A. Ojalvo, and A. Requena, J. Chem. Phys. **84**, 5077 (1986), and references cited therein.
and G. Karlström, J. Phys. Chem. **89**, 2171 (1985).
[31] M. R. A. Blombeg, U. B. Brandemark, I. Panas, P. E. M. Siegbahn, and U. Wahlgren, *Quantum Chemistry: The Challenge of Transition Metals and Coordination Chemistry*, NATO ASI Series, Series C, Vol. 176, edited by A. Veillard (Reidel, Dordrecht, 1986), pp. 11–14.
[32] See, e.g., A. Szabo and N. S. Ostlund, *Modern Quantum Chemistry: Introduction to Advanced Electronic Structure Theory* (MacMillan, New York, 1982).
[33] P. Karafiloglou and J. P. Malrieu, Chem. Phys. **104**, 383 (1986).
[34] (a) M. Merchán, R. González-Luque, I. Nebot-Gil, and F. Tomás, Chem. Phys. Lett. **112**, 412 (1984); (b) R. González-Luque, M. Merchán, I. Nebot-Gil, F. Tomás, and R. Montañana, J. Mol. Struct. Theochem. **121**, 57 (1985); (c) M. Merchán, R. González-Luque, I. Nebot-Gil, and F. Tomás, Chem. Phys. Lett. **114**, 516 (1985); (d) M. Merchán, J. Andrés, I. Nebot-Gil, E. Silla, and F. Tomás, J. Phys. Chem. **89**, 4769 (1985).
[35] C. M. Rohlfing and P. J. Hay, J. Chem. Phys. **83**, 4641 (1985), and references cited therein.
[36] (a) P. S. Bagus, C. J. Nelin, and C. W. Bauschlicher Jr., Phys. Rev. B **28**, 5423 (1983); (b) P. S. Bagus, K. Hermann, and C. W. Bauschlicher Jr., J. Chem. Phys. **80**, 4378 (1984).
[37] C. W. Bauschlicher Jr. and P. S. Bagus, J. Chem. Phys. **81**, 5889 (1984).
[38] (a) A. T. Amos and G. G. Hall, Proc. R. Soc. London Ser. A **263**, 483 (1961); (b) R. L. Martin and E. R. Davidson, Phys. Rev. A **16**, 1341 (1977).
[39] J. Koutecký, G. Pacchioni, and P. Fantucci, Chem. Phys. **99**, 87 (1985).
[40] A. B. Rives and R. F. Frenske, J. Chem. Phys. **75**, 1293 (1981).
[41] P. S. Bagus, K. Hermann, and C. W. Bauschlicher Jr., J. Chem. Phys. **81**, 1966 (1984).

Downloaded 29 Jan 2010 to 147.156.182.23. Redistribution subject to AIP license or copyright; see http://jcp.aip.org/jcp/copyright.jsp